Available online at www.sciencedirect.com
ScienceDirect
Biochimica et Biophysica Acta 1768 (2007) 3182–3192
Biochimica et Biophysica Acta
BBA
www.elsevier.com/locate/bbamem

Structural biology of membrane-acting peptides: Conformational plasticity of anticoccidial peptide PW2 probed by solution NMR

C. Cruzeiro-Silva [a,1], F. Gomes-Neto [a,1], L.W. Tinoco [b], E.M. Cilli [c], P.V.R. Barros [d], P.A. Lapido-Loureiro [d], P.M. Bisch [d], F.C.L. Almeida [a,*], A.P. Valente [a,*]

[a] *Centro Nacional de Ressonância Magnética Nuclear Jiri Jonas, Programa de Biologia Estrutural, Instituto de Bioquímica Médica, Universidade Federal do Rio de Janeiro, Rio de Janeiro, Brasil*
[b] *Nucleo de Produtos Naturais–Universidade Federal do Rio de Janeiro, Rio de Janeiro, Brasil*
[c] *Universidade Estadual Paulista, UNESP, Araraquara, São Paulo, Brasil*
[d] *Instituto de Biofísica Carlos Chagas Filho–Universidade Federal do Rio de Janeiro, Rio de Janeiro, Brasil*

Received 29 June 2007; received in revised form 22 August 2007; accepted 24 August 2007
Available online 6 September 2007

Abstract

The bottleneck for the complete understanding of the structure–function relationship of flexible membrane-acting peptides is its dynamics. At the same time, not only the structure but also the dynamics are the key points for their mechanism of action. Our model is PW2, a TRP-rich, cationic peptide selected from phage display libraries that shows anticoccidial activity against *Eimeria acervulina*. In this manuscript we used a combination of several NMR techniques to tackle these difficulties. The structural features of the membrane-acting peptide PW2 was studied in several membrane mimetic environments: we compared the structural features of PW2 in SDS and DPC micelles, that were reported earlier, with the structure properties in different lipid vesicles and the peptide free in water. We were able to unify the structural information obtained in each of these systems. The structural constraints of the peptide free in water were fundamental for the understanding of plasticity necessary for the membrane interaction. Our data suggested that the WWR sequence is the region responsible for anchoring the peptide to the interfaces, and that this same region displays some degree of conformational order in solution. For PW2, we found that affinity is related to the aromatic region, by anchoring the peptide to the membrane, and specificity is related to the N- and C-termini, which are able to accommodate in the membrane due to its plasticity.

1. Introduction

1.1. General remarks

Protein structural determination is a crucial way to fully understand the mechanism of action in biological events. The vast number of protein and nucleic acid structures is proving this affirmative accurate. However, structure determination of membrane proteins is still a challenge for structural biologists. Around 30% of the total proteins in the cell are membrane proteins but only a few representatives (less than 100) have their structure solved. They are less than 0.5% of the coordinates in the protein data bank.

Several techniques are contributing to improve this scenario. Among them are X-ray crystallography [1], solution NMR [2], solid-state NMR of oriented static samples of membrane protein in planar phospholipid bilayers [3,4] and magic angle spinning solid-state NMR of membrane protein incorporated in phospholipid vesicles [5]. The technical difficulties to get the structure of integral membrane lie on the high hydrophobicity. It turns protein expression demanding and expensive. Crystallization and NMR sample preparation are also challenging. Nonetheless, once the samples are prepared and the data acquisition is efficient, the final results are usually very satisfactory to explain the protein function and mechanism of action, which are the ultimate goal.

* Corresponding authors.
E-mail addresses: falmeida@cnrmn.bioqmed.ufrj.br (F.C.L. Almeida), valente@cnrmn.bioqmed.ufrj.br (A.P. Valente).
[1] Both authors contributed equally to the work.

0005-2736/$ - see front matter © 2007 Elsevier B.V. All rights reserved.
doi:10.1016/j.bbamem.2007.08.022

Membrane-acting peptides are usually less hydrophobic and smaller than integral membrane proteins and can be obtained in large quantities, many times by chemical synthesis [6]. However, the final structure obtained is frequently not able to fully explain its biological function. The reason is that membrane-acting peptide displays plastic and dynamic structures and they can accommodate differently in diverse membrane mimetic systems [6–16]. Here we present a strategy to study this very important class of macromolecules that can help the studies of membrane proteins.

1.2. Antimicrobial peptides

Antimicrobial peptides (AMPs) are spread in nature and are synthesized in organisms from both the vegetal and animal kingdoms and are among the most ancient host defense factors, which constitute the first line of defense and are involved in innate immunity [6,8].

The positive charge at physiological pH of AMPs is related to the initial interaction with the anionic head groups of the microbial phospholipids and the hydrophobic properties enable interaction of the peptide into the hydrophobic core of the membrane [7–16]. Recently, different evidences have shown that the membrane damage is only one of several mechanisms involved [11,17]. But still, the first step of AMPs mechanism of action is membrane interaction. Microbes that are able to change the charge of the membrane, by including positive charged compounds, became resistant to the AMPs [9,10]. Therefore, the first target for AMPs is believed to be the membrane but the precise mechanism of peptide uptake and cell membrane disruption that led ultimately to microbe death, is unknown [11,12].

AMPs have been considered good candidates for new antibiotic lead compounds. The impact in infectious diseases in human health is unquestionable and dramatic [6]. The appearance of infectious agents like HIV (AIDS), *Legionella pneumophila* (Legionnaire's disease), *Borrelia burgdorferi* (Lyme's disease) and recently SARS, and also the re-emergence of tuberculosis have stimulated the scientific community to develop new antibiotics. It is worth to mention that there is also an increase in microorganism resistance to the commonly used antibiotics [11].

Structural biology is very important for the development of new drugs. The possibility of mapping specific sites of interaction at the atomic level is outstanding in the new tools now available for the scientific community. The structure determination by X-ray and NMR is now common and can help in the elucidation of different system features.

NMR can also help us in answering some of the important questions for a successful rational drug design study [18]. First it can determine the structure at atomic level and give insights about important groups for interaction. In the case of peptides it can give even more important information: the dynamic of the peptide in the bound and free form. The molecular dynamics has helped in the development of flexible ligands and represents an important strategy for designing compounds. Nevertheless, experimental data can add structural features to speed-up drug reasoning.

1.3. Anticoccidial peptide PW2

PW2 was selected from phage display libraries through an alternative panning method using living sporozoites of *Eimeria acervulina* as target [19]. Synthetic PW2 (HPLKQYWWRPSI) shows anticoccidial activity against *E. acervulina* and *Eimeria tenella* with very low hemolytic activity. It also displays antifungal activity but no antibacterial activity. *Eimeria* is responsible for coccidiose, one of the most important diseases of domestic poultry. PW2 can damage *Eimeria* membrane of living cells and have no effect to other cells including from chicken intestine. Although, PW2 is a non-natural peptide, it shares features with antimicrobial peptides (AMPs): cationic properties due to the presence of Arg and Lys residues and amphipatic character [10,12].

In order to evaluate important features for PW2 membrane interaction, our laboratory determined the structure of PW2 by NMR in different micelles: sodium dodecylsulphate (SDS) and dodecylphosphocholine (DPC) [20,21]. The CD spectra of PW2 recorded in aqueous solution present a negative band at ~200 nm typical of random coil conformation. The addition of SDS, DPC and lipids led to a gain in the structure. SDS and DPC are commonly used for solution NMR studies of membrane protein resulting spectra with sharp lines. Also, DPC presents head group similar to membrane phospholipids. Both are available perdeuterated commercially and therefore we decided to evaluate PW2 structure in both systems as they give complementary structural information.

In SDS micelles, structural calculation shows that Trp7 forms a mini hydrophobic core that is important for the peptide folding [20]. The residues involved in the hydrophobic core are Trp7 in the center, Pro2 and Leu3 from the N-terminal region, and Pro10 from the C-terminal region. Lys4, Tyr6, Trp8 and Arg9 are in the same surface, possibly facing the micelle interface. This possibility is supported by the fact that chemical shift differences for theses residues were more pronounced when compared with PW2 in water and SDS. Trp7, Trp8 and Arg9 composed the WW+ consensus found in the sequence of the peptides selected with phage display [19]. These results suggest that Trp7, Trp8 and Arg9 are key residues not only for the peptide interaction with SDS but also for the interaction with *E. acervulina* sporozoites surface (Fig. 1A).

PW2 in DPC micelles also gains structure [21]. DPC forms zwitterionic interface and shares the phosphocholine polar head group with natural lipids [22]. PW2 structure in DPC displays two distinct regions: (i) the N-terminal 3–10 amphipatic helix (Leu3-Lys4-Gln5-Tyr6) and (ii) the aromatic region (Tyr6-Trp7-Trp8-Arg9) (Fig. 1B). The N-terminal region is folded as an amphipatic 3–10 helix, with intense NN(i, i+1) NOEs, several αN(i, i+2) and αN(i, i+3) and also absence of αN(i, i+4) NOEs. Several other medium range NOEs, that are typical of helix, stabilize this secondary structure.

Comparison of the structures obtained in SDS and in DPC (Fig. 1A and B) revealed important conformational changes between the two interfaces. The analysis of the structures highlights three important regions in the peptide: (i) the aromatic region that contains the consensus sequence of the phage display

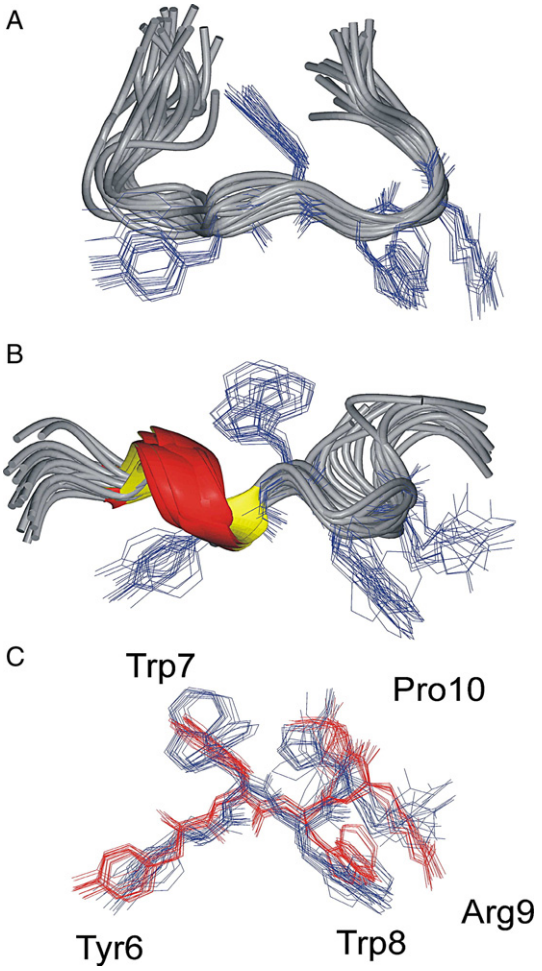

Fig. 1. Ribbon representation of the structures ensemble of PW2 in SDS micelles (A) [12] and in DPC micelles (B) [13]. The heavy atoms of the side chains of the residues within the aromatic region are shown in blue. The protein data bank code for the structure in SDS is 2HMY and in DPC is 2JQ2. (C) Superposition of the aromatic region of the structures in SDS (red) and DPC (blue).

WW+ that is shown to participate in the interaction with the interfaces of SDS and DPC micelle; (ii) the N-terminal region that is folded as an amphipatic 3–10 helix in DPC and is participating of the hydrophobic core in SDS; and (iii) the C-terminal region formed by the residues Ser11 and Ile12 that is not well structured, both in SDS and DPC.

In the present manuscript, to better understand the interaction with the interface, we studied PW2 free in solution and in the presence of phospholipid vesicles. To study it free in solution we used PW2 attached to a paramagnetic probe as its flexibility hampered the obtainment of NOEs and for the studies in vesicles, we applied the transfer NOE technique [23].

Our approach enabled a more complete understanding of PW2. We suggested that the plasticity of the membrane-acting PW2 peptide resides in the N- and C-terminal, while the WW+ motif shares similar features in all media. The presence of ordered conformation in the aromatic region of PW2 in water can be important to decrease the entropic penalty of binding. Moreover, the combination of structural features gave insights of how this small molecules exhibit specificity.

2. Materials and methods

2.1. Sample preparation of PW2

The peptide PW2 was synthesized commercially by Genemed Synthesis Inc. The lyophilized PW2 was solubilized in 20 mM sodium phosphate buffer (pH 5.0) containing 50 mM sodium chloride, 10% D_2O (99.9%, Isotec, Inc.). The final samples were 0.2, 0.5 and 4 mM in PW2.

2.2. Sample preparation of TOAC (2,2,6,6-tetramethylpiperidine-1-oxyl-4-amino-4-carboxilic acid)-PW2

The peptide TOAC-PW2 was manually synthesized based on the Fmoc chemistry solid-phase method. The incorporation of the paramagnetic probe was in the N-terminus. The lyophilized TOAC-PW2 was solubilized in 20 mM sodium phosphate buffer (pH 5.0) containing 50 mM sodium chloride, 10% D_2O (99.9%, Isotec, Inc.). The final sample concentrations were 0.1, 0.2, 0.4, 0.5 and 2 mM of TOAC-PW2.

2.3. NMR spectroscopy

NMR spectra were recorded on a Bruker Avance DRX600 and DRX400 operating at 600.04 and 400.13 MHz, respectively. The sample temperature was maintained at 25 °C. TOCSY spectra (spin-lock time of 70 ms) were acquired using the MLEV-17 pulse sequence [24]. Water suppression was achieved using the WATERGATE technique [25], and the spectra were collected with 512 data points in F1 and 4096 data points in F2 with 16 transients. The NMR data were processed with NMRPIPE [26].

2.4. Transfer-NOESY experiments

2.4.1. Preparation of unilamellar vesicles stock solution

The egg chicken lipids L-α-phosphatidylcholine (PC) and L-α-phosphatidylethanolmaine (transphosphatidylated) (PE) were purchased from Avanti Polar Lipids. The lipid powder was solubilized in chloroform in a molar ratio of 1:1. The PC:PE (1:1) solution was dried in nitrogen flux and then resuspended in buffer (20 mM sodium phosphate pH 5.0, 50 mM NaCl) to final concentration of 13.3 μM. Unilamellar vesicles were prepared by the extrusion method [27,28]. Lipid suspensions were extruded 40 times through a 0.22-μm polycarbonate filter. The vesicles were used immediately after preparation.

2.4.2. NMR sample preparation

A stock solution was prepared solubilizing PW2 in phosphate buffer (20 mM sodium phosphate pH 5.0, 50 mM NaCl) to final concentration of 4 mM. The NMR sample of PW2 solution in absence of vesicles was prepared by the dilution of the stock solution in phosphate buffer to final concentration of 2 mM including 10% (v/v) of deuterium oxide.

The NMR sample of PW2 peptide solution in the presence of vesicles was prepared by dilution of PW2 stock solution in phosphate buffer to final concentration of 2 mM. Added the vesicle stock solution to the final concentration of 5 mM of lipids including 10% (v/v) deuterium oxide.

TOCSY spectra using MLEV (spin-lock time of 25 ms) were acquired at 600.04 MHz, with 64 scans, 4096 complex points in F2 and 512 complex points in F1. The spectral width was 12 ppm in both dimensions. We used digital quadrature detection in F2 and States TTPI in F1. Water suppression was achieved using the 3–9–19 pulse sequence with gradients [29].

NOESY spectra (mixing time of 50 ms, 80 ms, 90 ms and 120 ms) were acquired at 600.04 MHz, with 64 scans, 4096 complex points in F2 and 512 complex points in F1. The spectral width was 12 ppm in both dimensions. We used digital quadrature detection in F2 and States TTPI in F1.Water suppression was achieved using the 3–9–19 pulse sequence with gradients [29].

The NMR spectra were analyzed using NMRVIEW, version 5.04 [30]. NOE cross-peaks were integrated in the NOESY spectra, and their volumes were converted to distances, which were calibrated using the equations suggested by Hyberts et al. [31]. The structure calculations were performed using CNS_Solve version 1.1 [32]. All the structures were analyzed with the program MOLMOL [33].

2.5. Relaxation experiment

All relaxation experiments were measured at 600.04 MHz. The spin–lattice relaxation was acquired using the inversion–recovery pulse sequence [34]. The frequency dependence of proton spin–lattice relaxation rate (T1) has been measured in amide region. The transverse relaxation time was acquired using the CPMG (Curr–Purcell–Meiboom–Gill) pulse sequence [35]. The frequency dependence of proton transverse relaxation rate (T2) has been measured in amide region.

2.6. Paramagnetic relaxation enhancement (PRE)

Different from distances measured by NOEs, the effect of an unpaired electron on the relaxation of hydrogen extends to the range up to 20 to 25 Å. The interaction of a free electron with hydrogen is described by the Solomon–Bloembergen equations [36–39], which describe the enhancement of the hydrogen's longitudinal ($R1$) and transverse ($R2$) relaxation rates:

$$\Delta R1 = (2K(3\tau_c/(1+\omega_H^2\tau_c^2)))/r^6 \quad (1)$$

$$\Delta R2 = K(4\tau_c + 3\tau_c/(1+\omega_H^2\tau_c^2)))/r^6 \quad (2)$$

The constant K for a nitroxide radical is 1.23×10^{-32} cm^6 s^{-2}, ω_H is the Larmour frequency of the hydrogen, r is the distance between the free electron and the proton, τ_c is the correlation time for the electron-proton vector.

The equations assume isotropic rotational diffusion of the free electron-hydrogen vector. These equations have been used to calculate time average values of r in denatured protein [38,39].

The value of τ_c was estimated from the ratio $\Delta R2/\Delta R1$ using the following approximation, valid when $\omega_H\tau_c > 1$:

$$\tau_c = ((6(\Delta R2/\Delta R1) - 7)/4\omega_H^2)^{1/2}. \quad (3)$$

2.7. Molecular dynamics simulations

All the molecular dynamics simulations (MD) were performed using GROMACS 3.3.1 software [40], with the OPLS-AA/L all-atom force field [41].

The peptide was solvated with 6471 water Simple Point Charge (SPC216) [42] molecules with a triclinic box (minimum distance between the solute and the box of 1.2A). Two chlorine counter ions (2 Cl$^-$) were added, replacing water molecules randomly in the box, to neutralize the positive charges on peptide.

Prior to the MD simulation, the system was relaxed by energy minimization using 20,000 steps of SteepDescent under position restraints, 20,000 steps of SteepDescent and 20,000 of Conjugated Gradients. The temperature was increased slowly, 100 ps of MD at 50 K, 100 K, 150 K, 200 K, 250 k and 298 K. The equilibrium simulation ran during 10 ns at 298 K.

During the MD simulation, the LINCS algorithm [43] was used to constrain the lengths of covalent bonds. The time step for the simulations was 2 fs. The simulations were run under constant pressure and temperature, using Berendsen's coupling algorithm [44]. VDW forces were treated using a cutoff of 1.2 nm. Long-range electrostatic forces ($r > 1.2$ nm) were treated using the particle mesh Ewald method [45].

2.8. R1ρ relaxation dispersion

The rotating frame relaxation rate ($R1\rho$) was recorded on a Bruker Avance DRX400 operating at 400.13 MHz. The sample temperature was maintained at 25 °C and the concentration of PW2 was 200 μM. The sample conditions were the same described above.

The rotating-frame relaxation rate ($R1\rho$) was measured using the following one-dimensional basic pulse sequence [46]:

$$\pi/2(\phi 1) - \{\pi/2(\phi_2) - \tau\}_n - \pi/2(\phi_1) - \mathrm{PFG}(z) - \pi/2(\phi_1) - \mathrm{acq}(\phi_{rec})$$

The phase cycle was $\phi_1 = x, -x, -x, x, y, -y, -y, y$, $\phi_2 = -y, y, y, -y, x, -x, -x, x$ and $\phi_{rec} = x, -x, -x, x, y, -y, -y, y$. The pulsed field gradient (PFG) in z was set for 1 ms at 8 G/cm. The spin lock was achieved adjusting the delay τ, according to the duty cycle necessary to produce the desired spin lock field strength. n was the loop to adjust the total time for spin lock. We used a hard pulse of 25.9 kHz. The ^{1}H carrier frequency was adjusted in the middle of the amide region during the spin lock, so the off resonance effect can be neglected. Water suppression was achieved by presaturating the water resonance.

3. Results

PW2 free in solution is very flexible and displays CD spectrum typical of random coil conformation [20]. The NOESY spectrum did not display interesidue NOEs and the scalar coupling values are also compatible with a flexible structure. To evaluate PW2 structural features in solution we used a paramagnetic probe TOAC (4-amino-2,2,6,6-tetramethylpiperidine-1-oxyl-4-carboxylic acid [47,48]). This nitroxide probe can be attached by chemical synthesis in the N-terminal and the linkage resembles a peptide bond ([47], Fig. 2). The paramagnetic properties of TOAC can then be used to evaluate the structural tendency of the peptide by the study of the relaxation parameters. The advantage of paramagnetic probe is that the range of action is higher than NOEs because the gyromagnetic ratio of a free electron is near three orders of magnitude higher than that of a proton [36–39]. Therefore, even in a peptide that does not adopt a rigid structure, the paramagnetic effect can give structural information since transient contacts can be observed. Paramagnetic relaxation enhancement (PRE) is sensitive to the distance between the proton and the free electron of the spin label providing quantitatively measurements of average distances. PRE has been used to study molten globule and unfolded proteins with great success [38,39].

Fig. 3 shows the ^{1}H 1D spectra of PW2 and TOAC-PW2. The chemical shift dispersion is similar but the resonances are broader due to the paramagnetic effect in TOAC-PW2. The TOAC-PW2 was assigned by comparison with the peptide without TOAC. Peaks corresponding to His1 were broad beyond detection, an expected result due to the probe position.

Chemical shift difference between PW2 and TOAC-PW2 is presented in Fig. 4 showing a larger difference in the N- and C-terminal. With the exception of Leu3 the highest chemical shift change was lower than 0.04 ppm. All the spectra are the

Fig. 2. Primary sequence of TOAC-PW2, showing the paramagnetic probe TOAC [37,38].

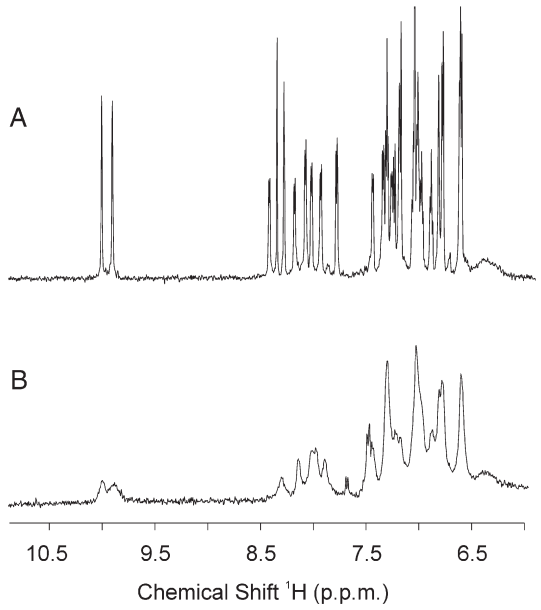

Fig. 3. ^{1}H one-dimensional NMR spectra of the amidic and aromatic regions of PW2 (A) and TOAC-PW2 (B), both in water. Note that the chemical shifts are similar but the lines are broader in the spectrum of TOAC-PW2.

same despite the peptide concentration suggesting that no aggregation is responsible for the results.

The quantitative analysis of the paramagnetic effect was obtained by measuring the relaxation parameters for PW2 and TOAC-PW2 as described by Gillespie and Shortle [38]. Supplementary Fig. 1 shows $R1$ and $R2$ values for PW2 at two concentrations (200 μM and 500 μM). One important aspect is that the values of $R2$ are always higher than the values of $R1$, showing that the extreme narrowing limit has been surpassed. We used the amide proton to quantify the average distance to the paramagnetic probe and the values of $\Delta R1$ and $\Delta R2$ are presented in Fig. 5 for the two samples. Similarly to the chemical shift difference, PRE was more pronounced in the N- and C-terminal.

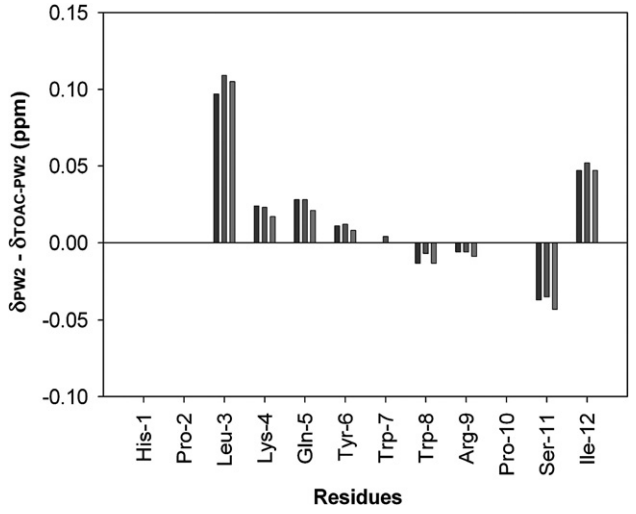

Fig. 4. Chemical shift difference between the unlabeled PW2 (4 mM) and TOAC-PW2 at 500 (dark gray), 400 (gray) and 200 μM (light gray). The difference does not change with concentration suggesting that PW2 does not aggregate. The paramagnetic effect is more pronounced in the N- and C-terminals.

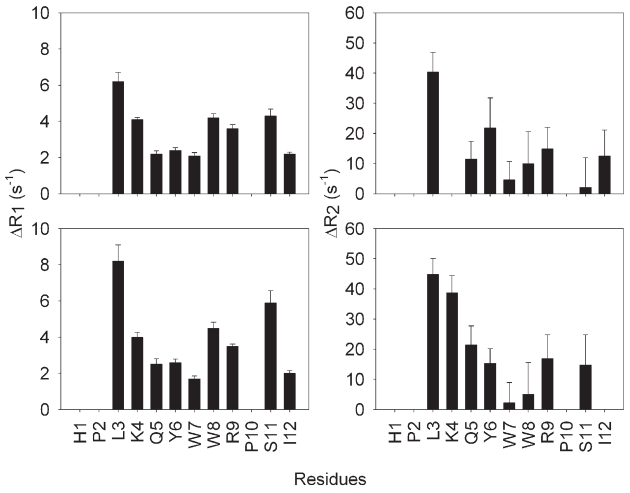

Fig. 5. Difference between measured $R1$ and $R2$ of TOAC-PW2 and unlabeled PW2 as a function of residue name. The error bars indicate the sum of fitting error of the relaxation measurements of PW2 and TOAC-PW2. The experiments were done in triplicate.

All relaxation parameters were compiled to calculate the time average distance as described in Materials and methods. Table 1 shows the average distance of each amide hydrogen and the rotational correlation time (τ_c) for the vector between the free electron and each amide. The observed τ_c has a minor component of the longitudinal relaxation rate of the electron, but is predominantly dominated by the effective rotational correlation time of the vector [36–38]. The average distances obtained at 200 μM and 500 μM of PW2 concentration are in agreement, meaning that there is not a concentration effect that might suggest peptide aggregation.

The values of τ_c were calculated from Eq. (3). This equation is valid when τ_c is in the nanosecond time scale, because then

Table 1
Summary of the calculated parameters from data of paramagnetic relaxation enhancement obtained for TOAC-PW2 in water

Residue	τ_c (seconds)	Distance (0.2 mM) (Å)	Distance (0.5 mM) (A)	Distance (Å)
His1	–	–	–	–
Pro2	–	–	–	–
Leu3	4.5e−9	13.5	13.1	13.3
Lys4	6.0e−9	–	14.1	14.1
Gln5	4.8e−9	16.4	15.5	15.9
Tyr6	5.1e−9	15.4	15.8	15.6
Trp7	1.4e−9	17.1	18.5	17.8
Trp8	2.2e−9	15.5	16.4	15.9
Arg9	3.7e−9	15.4	15.3	15.3
Pro10	–	–	–	–
Ser11	2.4e−9	17.8	14.6	16.2
Ile12	4.3e−9	16.2	20.9	18.6

τ_c is the rotational correlation time of the vector between the free electron and each amide hydrogen. The distances were calculated from Eqs. (2) and (3) for the two concentrations [28].

$\omega_H\tau_c > 1$. This was the case for PW2 free in water. Most of the values of τ_c are larger than 1.6 ns where the extreme narrowing limit is surpassed. The lower value obtained for τ_c was for Trp7. It is worth mentioning that the distance presented in Table 1 was calculated using Eqs. (1) and (2) using the values of τ_c for each residue. However if we calculate the distances using fixed values of τ_c (from 1 to 6 ns), the resulting distances vary in less than 1 Å from the distances showed in Table 1. We considered the calculations satisfactory for the qualitatively analysis of the distances used in this manuscript.

The expected τ_c for a hypothetical folded state of PW2 in water was estimated to be 1.6 ns. This value was found for the structure of PW2 in SDS using the software HYDRONMR [49]. The value obtained for Trp7 was the smallest value observed for τ_c, suggesting that this residue displays the most restricted motion. The values of τ_c are also low for Trp8, Arg9 and Ser11. The other residues showed higher values of τ_c, reaching 6 ns, meaning that the peptide chain is undergoing less restricted motion and behaving as an unfolded protein.

We also compared the average distances (Table 1) obtained from PRE with extended, random and the well-folded structures of PW2 in SDS and DPC (Fig. 1). Using CNS_solve, we generated a low-energy extended conformation of PW2 and 800 random structures. We generated four sets of 200 random coil structures. 200 for each possible combination of proline 2 and 10 (*cis–trans* isomerization: *trans–trans*, *trans–cis*, *cis–trans*, *cis–cis*). Fig. 6 shows the comparison of the average distances obtained with PRE (Table 1) and the distances of each amide proton and the ε1-hydrogen of His1. When the comparison was done with the random (Fig. 6A) and extended (Fig. 6B) conformations, clearly the results did not match. In both random coil and the extended peptide the average distances increase with the primary structure position, while in the PRE results have an inverted U-shaped curve.

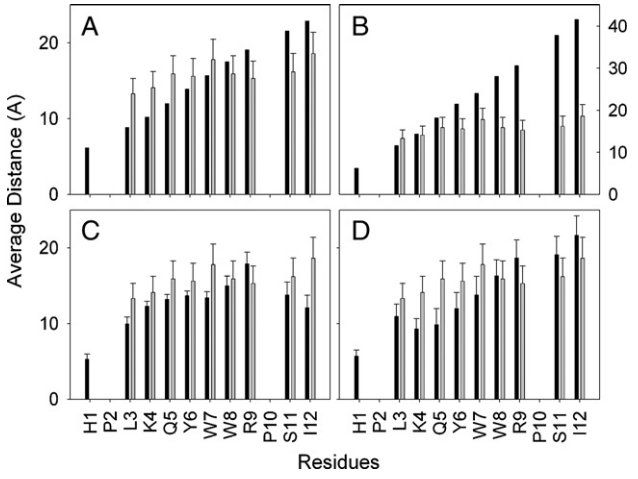

Fig. 6. Average distances calculated from PRE (gray) for each residue of PW2. The bars in black represent the distance measured from each amide hydrogen and ε1 hydrogen of histidine 1, in several PW2 structures: (A) average distance measured in 800 random structures of PW2, minimized extended structure of PW2 (B), structure ensemble of PW2 in SDS (C) [12] and structure ensemble of PW2 in DPC (D) [13]. The calculated distances were not compatible with random or extended conformation (A). However, the distances are comparable to the ones obtained from the NMR structures of PW2 in SDS (B) and DPC (C) micelles. Our data suggest a curvature in the peptide that could be similar to the results in SDS and DPC.

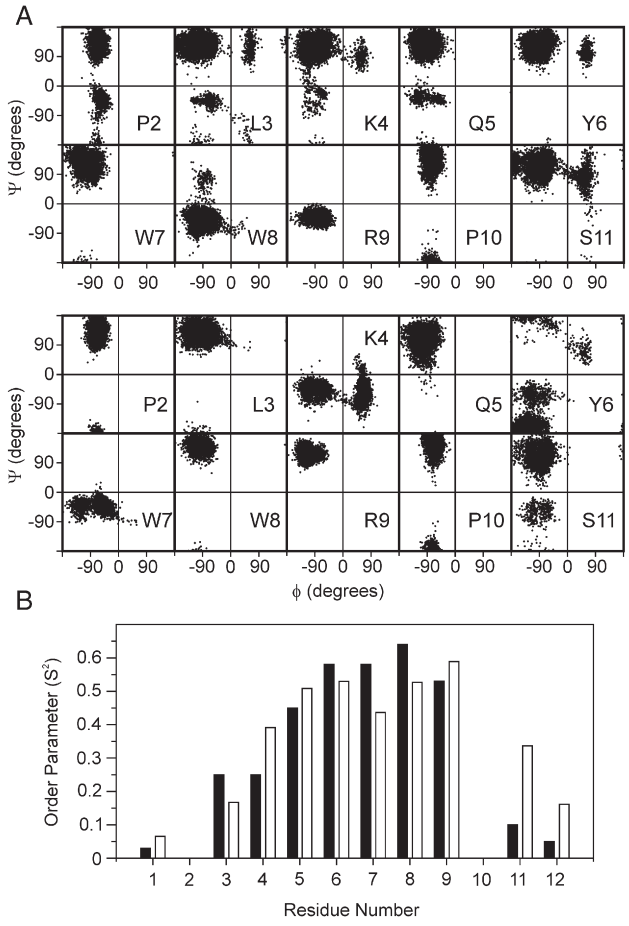

Fig. 7. Ramachandran plot of the MD trajectory for each residue of PW2 in a water box. (A) MD simulation starting from the lower energy structure obtained in SDS [12]; and (B) starting from the lower energy structure of PW2 in DPC. The order parameters of the NH bond vector for the 10 ns MD are shown in panel C. Black bars represent the order parameter for the MD starting from the structure in SDS, while white bars represent the order parameter for the MD starting from the structure in DPC. Both MD simulations indicated a higher degree of order for the residues within the aromatic region.

Remarkably, when the average distances obtained with PRE are compared to the calculated structures obtained in SDS and DPC the values could be correlated (Fig. 6C and D). These data suggest that although the peptide is flexible in aqueous solution, the N- and C-termini of the peptide were transiently closed. The WW+ motif is composed by large side chains and possibly reduces the flexibility of the whole peptide chain.

To confirm this idea, we performed molecular dynamic simulation (MD) of the PW2 in a water box starting from the structures solved in SDS and DPC [20,21]. Since in the MD the peptide is unrestrained, structural segments that are not stabilized by internal tertiary contacts or sterical effects will lose its structure during the MD trajectory of 10 ns. Fig. 7 shows the trajectory of phi and psi torsion angle (Ramachandran plots) for each amino acid. The residues within the aromatic region started and ended the MD in the same region of the Ramachandran, while the other amino acids, composing the N- and C-termini

visited several regions. The WW+ motif displays restrained motion in aqueous solution. Fig. 7B shows the order parameter (S^2) for the NH bond vector calculated for each residue from the MD trajectory. Note that the aromatic region displays the highest degree of order in the peptide. A higher degree of order is expected in the middle of any polypeptide chain. For PW2 we observed that the residues displaying higher order parameters are shifted toward the C-terminal portion, from residues 6 to 10. We believe that the occurrence of amino acids with large side chain enforces a restriction in the chain movement. We observed similar behavior starting the MD simulations from PW2 structures in SDS and DPC.

Both the experimental data of PRE and the MD simulations point to the presence of ordered conformational state of PW2 free in water. MD simulation suggested that the ordered residues are within the aromatic region. However we wanted an experimental approach to map the ordered region. Relaxation dispersion experiments are a tool that enables the mapping of residues that undergo motions in the milli- to microsecond time scale [46]. Interconversion between low-energy states of the energy landscape of a protein results in backbone motions within this time scale [50]. Fig. 8 displays the relaxation dispersion curve for each residue of PW2 free in water. The backbone of Leu3, Gln5, Tyr6 and Trp7 showed the highest amplitude changes of $R1\rho$ as a function of spin lock field strength. This was also true for Trp7 and Trp8 side chains. These residues are the most affected by milli- to microsecond time scale motions, strongly suggesting that these residues are involved in the conformational exchange among ordered states of PW2 in water.

3.1. Structural features of PW2 in lipid vesicles

We found that the PW2 aromatic region, which displays similar structure in SDS and DPC (Fig. 1C), is also ordered in water, suggesting that this is an anchoring region of the peptide to the interface. The N-terminal region, which behaved as an unfolded polypeptide chain in solution, displayed different structures in SDS and DPC. The plasticity of this region seems to be important for the environmental dependence of PW2 structure, and ultimately to the specificity toward different interfaces. However we do not know if the same rationalization applies for lipid bilayers. Although the chemical nature of the head groups can be the same as DPC, the dynamics of lipid bilayers are very different from the one of micelles. In micelles the time scale for exchange of a monomer of the detergent is in the microsecond range. In lipid bilayers this time scale ranges from minutes to hours [51].

Therefore, we decided to study the effect of phosphatidylcholine (PC) vesicles and a mixture PC and phosphatidylethanolamine (PE) vesicles (1:1) on the structure of PW2. We

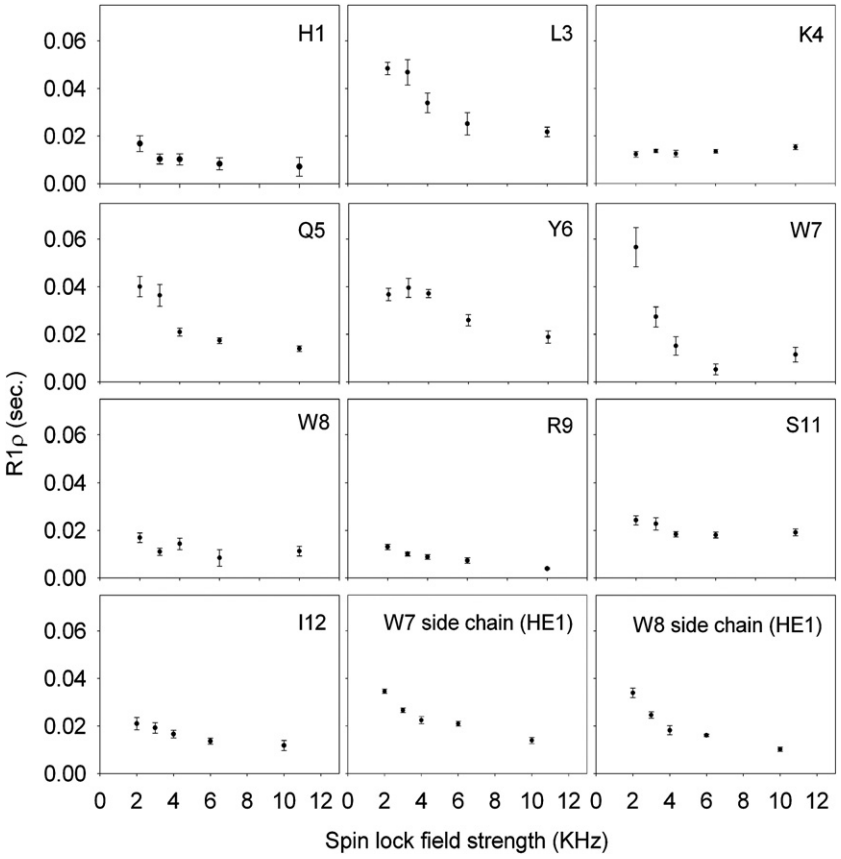

Fig. 8. $R1\rho$ of PW2 in water for each amino acid residue as a function of the spin lock field strength. These data show that PW2 in aqueous solutions undergoes motion in the time scale of milli- to microseconds. The presence of conformational exchange means that there is conformational diversity of the peptide corroborating the idea of ordered conformers in the free state. The residues that show more pronounced dependence of $R1\rho$ on spin lock field strength are Leu3, Gln5, Tyr6, Trp7 and the side chains of Trp7 and Trp8.

decided to use 1:1 ratio of PC: PE because PW2 is able to leak vesicles with this composition but not vesicles of PC alone (data not shown). We did not intend to mimic the parasite membrane but the influence of phospholipids in PW2 structural features.

We evaluated the spectra of PW2 in the presence of vesicles of PC and PCPE. In both cases, the spectra displayed sharp lines, suggesting that PW2 is either not interacting or interacting in fast exchange with the interface. To further understand the effect we acquired three NOESY spectra using short mixing times (<120 ms). Fig. 9A shows the NOESY spectra of PW2 in the absence of vesicles, and in the presence of PC and PCPE. The spectra of PW2 free in solution and in the presence of PC did not built up transfer NOEs, indicating that the peptide interacts weakly or does not interact with PC interface. Remarkably, the NOESY spectra in the presence of PCPE generated several transfer NOES in all mixing times. These data indicate the interaction of PW2 to PCPE interface.

Fig. 9B shows the analysis of the total number of NOEs per residue and the chemical shift perturbation caused by the transient interaction of PW2 with PCPE. We observed that the majority of the NOEs come from the aromatic region. Most of the NOEs are connecting hydrogens from aromatic side chains, suggesting that the aromatic region is getting structured in the bound conformation. We observed only few NOEs for the N-terminal region. With these data we suggest that the aromatic region is anchoring PW2 to PCPE.

The analysis of chemical shift perturbation is also informative. The biggest perturbation was found for Ile12 for both α and amide hydrogen. This indicates the participation of the C-terminal region in specific contact to PCPE interface. The other shifts observed are very small, restricting the analysis. How-

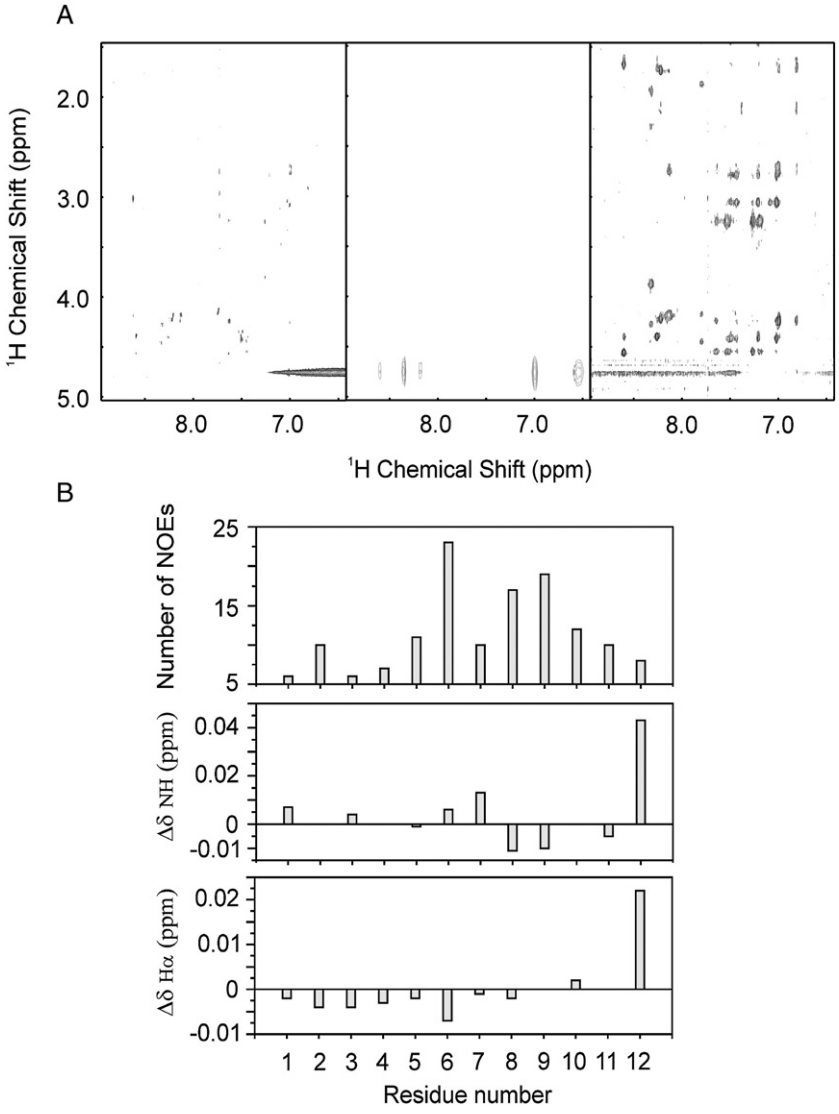

Fig. 9. NOESY spectra at a mixing time of 120 ms of PW2 in water (A left), in the presence extruded vesicles of PC (A center) and extruded vesicles of PCPE (A right). NOESY spectra in the presence of PCPE generated several transferred NOES in all mixing times. Panel B shows total number of NOEs for each residue of PW2 in PCPE (top), difference between the chemical shift of each amide hydrogen of PW2 in PCPE and in water (center), and difference between the chemical shift of each alpha hydrogen of PW2 in PCPE and in water.

ever, we observed chemical shift perturbation for the amide hydrogens on the aromatic region, confirming the participation of this region in the interaction, and for the α hydrogen in the N-terminal region. Any further interpretation would be speculative.

The transfer NOEs observed in Fig. 9A were enough to calculate a low-resolution structure. This structure was not presented here because it displayed high conformational averaging. We are now using restrained MD simulation and cross-validation of the NOEs to improve our capability to calculate such structures.

4. Discussion

The main goal of structural biology is to correlate molecular structure with biological function. Several systems were unveiled by the tertiary structure determination of its components. Important details about mechanism of action for these systems were obtained. However, for some systems there are features that are not fully understood due to the importance of dynamic in the process. Frequently, regions of binding are flexible and undergo conformational exchange [52–54].

A lot of progress is being done for the comprehension of the mechanism of action of membrane-acting peptides Antimicrobial peptides represent a class of peptide that act primary at the membrane. Despite the amphipatic character, there is not a clear structural feature that explains the site of membrane interaction or specificity. Actually, only a small number of amino acid positions are essential for antimicrobial activity [11]. All these features suggest that antimicrobial peptides have a large structural plasticity that is probably responsible for their ability to interact with different types of interfaces (specificity). Structure–function studies of antimicrobial peptides indicate that a number of parameters modulate antibiotic activity: conformation, charge distribution, hydrophobicity and amphipathicity [55].

In our studies of PW2 we tried to find which features may describe a binding region and which are the key amino acids. In the case of PW2 the aromatic region is probably the one responsible for primary interaction and the N- and C-termini are involved in membrane accommodation. Furthermore, we believe that the Trp side chain may restrict the backbone motion imposing a conformational exchange point for the whole chain, not only in the presence of interfaces but also when the peptide is free in solution.

Binding regions are frequently reported to have conformational exchange, instead of being completely flexible [56,57]. The binding regions are not well represented as a single well-defined state but should be described as several favorable conformations. The complex structural features of ligand binding regions represent a hindrance in computational drug design [58,59].

Several antimicrobial peptides present aromatic residues important for antimicrobial activity and tryptophan is frequently among them. The restriction around the tryptophans in PW2 may confer rigidity to minimize the entropic cost on binding, whereas surroundings residues form a flexible support [60,61]. Evidence that tryptophan imposes structural restrictions in peptides has been reported by other groups. Dames et al. [62] studied short peptides (9 aa) conformational preferences using residual dipolar couplings (RDCs). They observed that when tryptophan is present in the middle of the primary sequence (position 5 or 6) it creates a kink or a bulge of the peptide backbone, since the coil model fails to reproduce the $^{1}D_{\mathrm{CAHA}}$ RDCs [62].

Therefore, it seems that tryptophan has special features that may be important for the binding processes, probably related to the size of its side chain. Actually, presence of tryptophan residues in interaction interfaces is found in several protein complexes. Recently, Ma et al. [63] reported tryptophan is a conserved residue at the binding sites in macromolecule complexes. Furthermore, they found that similar residue hot spots occur across different protein families suggesting that affinity and specificity are not necessarily coupled [63]. For PW2, we found that affinity is related to the aromatic region, by anchoring the peptide to the membrane, and specificity is related to the N- and C-termini, which are able to accommodate in the membrane due to its plasticity.

It is worth to mention that tryptophan is also frequently found in membrane protein close to the interaction with the phospholipid polar head, mainly the phosphate group [64]. Therefore, tryptophan may represent a suitable hot spot of interaction not only for protein–protein but also protein–lipid interfaces.

Recently a new interpretation suggests that proteins exist as a family of conformations [50,52,65,66], and the conformation with biological activity is probably selected from a family of pre-existent structures [52]. The “biological conformation” is a product of the conformational diversity and the magnitude of difference can be from loop movement to secondary structure elements up to global rearrangement. Therefore, the measurement of structure dynamics is fundamental for understanding of phenomenon of molecular recognition.

We can then conclude that the aromatic region anchors PW2 to the membrane. This region is responsible for the first approximation with the membrane and probably to the affinity of the peptide to interfaces. The other regions of the peptide might be responsible to specificity and membrane destabilization. We do not know the exact features responsible for specificity, but it is likely that Ile12 is related to specificity, since it participates to the binding to PCPE vesicles. Specificity is also a function of the chemical nature of the interface. Most likely, substitution of PC by PE increases the exposure of the hydrophobic portion of the bilayer, due to the lower volume of PE polar head, facilitating then the interaction with Ile12.

Acknowledgments

We acknowledge the funds from the International Center for Genetic Engineering and Biotechnology (ICGEB, Trieste, Italy), Conselho Nacional de Desenvolvimento Científico e Tecnológico (PRONEX-CNPq, Brazil), Fundação Carlos Chagas Filho de Amparo à Pesquisa do Estado do Rio de Janeiro (FAPERJ, Brazil), Millennium Institute of Structural Biology in Biotechnology and Biomedicine.

Appendix A. Supplementary data

Supplementary data associated with this article can be found, in the online version, at doi:10.1016/j.bbamem.2007.08.022.

References

[1] P.J.L. Werten, H.W. Remigy, B.L. de Groot, D. Fotiadis, A. Philippsen, H. Stahlberg, H. Grubmuller, A. Engel, Progress in the analysis of membrane protein structure and function, FEBS Lett. 529 (2002) 65–72.

[2] L.K. Tamm, B.Y. Liang, NMR of membrane proteins in solution, Prog. Nucl. Magn. Reson. Spectrosc. 48 (2006) 201–210.

[3] S.J. Opella, F.M. Marassi, Structure determination of membrane proteins by NMR spectroscopy, Chem. Rev. 104 (2004) 3587–3606.

[4] A. Ramamoorthy, Y.F. Wei, D.K. Lee, PISEMA solid-state NMR spectroscopy advances in solid state NMR studies of materials and polymers: a special volume dedicated to Isao Ando, Ann. Rep. NMR Spectrosc. 52 (2004) 1–52.

[5] O.C. Andronesi, S. Becker, K. Seidel, H. Heise, H.S. Young, M. Baldus, Determination of membrane protein structure and dynamics by magic-angle-spinning solid-state NMR spectroscopy, J. Am. Chem. Soc. 127 (2005) 12965–12974.

[6] P. Bulet, R. Stöcklin, L. Menin, Anti-microbial peptides: from invertebrates to vertebrates, Immunol. Rev. 198 (2001) 169–181.

[7] U.H.N. Dürr, U.S. Sudheendra, A. Ramamoorthy, LL-37, the only human member of the cathelicidin family of antimicrobial peptides, Biochim. Biophys. Acta 1758 (2006) 1408–1425.

[8] V. Dhople, A. Krukemeyer, A. Ramamoorthy, The human beta-defensin-3, an antibacterial peptide with multiple biological functions, Biochim. Biophys. Acta 1758 (2006) 1499–1512.

[9] H. Sato, J.B. Feix, Peptide–membrane interactions and mechanisms of membrane destruction by amphipacthic α-helical antimicrobial peptides, Biochim. Biophys. Acta 1758 (2006) 1245–1256.

[10] A. Peschel, How do bacteria resist human antimicrobial peptides? Trends Microbiol. 10 (2002) 179–186.

[11] A. Peschel, H.G. Sahl, The co-evolution of host cationic antimicrobial peptides and microbial resistance, Nat. Rev., Microbiol. 4 (2006) 529–536.

[12] A. Ramamoorthy, S. Thennarasu, A. Tan, D.-K. Lee, C. Clayberger, A.M. Krensky, Cell selectivity correlates with membrane-specific interactions: a case study on the antimicrobial peptide G15 derived from granulysin, Biochim. Biophys. Acta 1758 (2006) 154–163.

[13] V. Dhople, A. Krukemeyer, A. Ramamoorthy, The human beta-defensin-3, an antibacterial peptide with multiple biological functions, Biochim. Biophys. Acta 1758 (2006) 1499–1512.

[14] A. Ramamoorthy, S. Thennarasu, D.-K. Lee, A. Tan, L. Maloy, Solid-state NMR investigation of the membrane-disrupting mechanism of antimicrobial peptides MSI-78 and MSI-594 derived from magainin 2 and melittin, Biophys. J. 91 (2006) 206–216.

[15] F. Porcelli, B. Buck, D.-K. Lee, K.J. Hallock, A. Ramamoorthy, G. Veglia, Structure and orientation of pardaxin determined by NMR experiments in model membranes, J. Biol. Chem. 279 (2004) 45815–45823.

[16] F. Porcelli, B. Buck, D.-K. Lee, S. Thennarasu, A. Ramamoorthy, G. Veglia, Structures of the dimeric and monomeric variants of magainin antimicrobial peptides (MSI-78 and MSI-594) in micelles and bilayers, determined by NMR spectroscopy, Biochemistry 45 (2006) 5793–5799.

[17] D.S. Lobo, I.B. Pereira, L. Fragel-Madeira, L.N. Medeiros, L.M. Cabral, J. Faria, M. Bellio, R.C. Campos, R. Linden, E. Kurtenbach, Antifungal *Pisum sativum* defensin 1 interacts with *Neurospora crassa* cyclin F related to the cell cycle, Biochemistry 46 (2007) 987–996.

[18] M. Pellecchia, D.S. Sem, K. Wuthrich, NMR in drug discovery, Nat. Rev. Drug Discov. 1 (2002) 211–219.

[19] A. da Silva, U. Kawazoe, F.F.T. Freitas, M.S.V. Gatti, H. Dolder, R.I. Schumacher, M.A. Juliano, M.J. da Silva, A. Leite, Avian anticoccidial activity of a novel membrane-interactive peptide selected from phage display libraries, Mol. Biochem. Parasitol. 120 (2002) 53–60.

[20] L.W. Tinoco, A. Da Silva Jr., A. Leite, A.P. Valente, F.C.L. Almeida, NMR structure of PW2 bound to SDS micelles. A tryptophan-rich anticoccidial peptide selected from phage display libraries, J. Biol. Chem. 277 (2002) 36351–36356.

[21] L.W. Tinoco, F. Gomes-Neto, A.P. Valente, F.C.L. Almeida, Effect of micelle interface on the binding of the anticoccidial PW2 peptide. J. Biomol. NMR (in press).

[22] T.L. Whitehead, L.M. Jones, R.P. Hicks, PFG-NMR investigations of the binding of cationic neuropeptides to anionic and zwitterionic micelles, J. Biomol. Struct. Dyn. 21 (2004) 567–576.

[23] C.B. Post, Exchange-transferred NOE spectroscopy and bound ligand structure determination, Curr. Opin. Struct. Biol. 13 (2003) 581–588.

[24] A. Bax, D.G. Davis, MLEV-17-based two-dimensional homonuclear magnetization transfer spectroscopy, J. Magn. Reson. 65 (1985) 355–360.

[25] M. Piotto, V. Saudek, V. Sklenar, Gradient-tailored excitation for single-quantum NMR-spectroscopy of aqueous-solutions, J. Biomol. NMR 2 (1992) 661–665.

[26] F. Delaglio, S. Grzesiek, G.W. Vuister, G. Zhu, J. Pfeifer, A. Bax, NMRPIPE — a multidimensional spectral processing system based on unix pipes, J. Biomol. NMR 6 (1995) 277–293.

[27] N.K. Subbarao, R.I. MacDonald, K. Takeshita, R.C. MacDonald, Characteristics of spectrin-induced leakage of extruded, phosphatidylserine vesicles, Biochim. Biophys. Acta 1063 (1991) 147–154.

[28] R.C. MacDonald, R.I. MacDonald, B.P. Menco, K. Takeshita, N.K. Subbarao, L.R. Hu, Small-volume extrusion apparatus for preparation of large, unilamellar vesicles, Biochim. Biophys. Acta 1061 (1991) 297–303.

[29] V. Sklenar, M. Piotto, R. Leppik, V. Saudek, Gradient-tailored water suppression for H-1-N-15 HSQC experiments optimized to retain full sensitivity, J. Magn. Reson., Ser. A 102 (1993) 241–245.

[30] B.A. Johnson, R.A. Blevins, NMRView—a computer-program for the visualization and analysis of NMR data, J. Biomol. NMR 4 (1994) 603–614.

[31] S.G. Hyberts, M.S. Goldberg, T.F. Havel, G. Wagner, The solution structure of Eglin-C based on measurements of many NOEs and coupling-constants and its comparison with X-ray structures, Protein Sci. 1 (1992) 736–751.

[32] A.T. Brunger, P.D. Adams, G.M. Clore, W.L. Delano, P. Gros, R.W. Grosse-Kunstleve, J.S. Jiiang, J. Kuszewski, N. Nilges, N.S. Pannu, R.J. Read, L.M. Rice, T. Simonson, G.L. Warren, Acta Crystallogr. Sect. D, Biol. Crystallogr. 54 (1998) D905–D921.

[33] R. Koradi, M. Billeter, K. Wüthrich, MOLMOL: a program for display and analysis of macromolecular structures, J. Mol. Graph. 14 (1996) 51–55.

[34] S. Meiboom, D. Gill, Modified spin-echo method for measuring nuclear magnetic relaxation times, Rev. Sci. Instrum. 29 (1958) 688–691.

[35] L.E. Kay, D.A. Torchia, A. Bax, Backbones dynamics of proteins as studied by ^{15}N inverse detected heteronuclear NMR spectroscopy: application to staphylococcal nuclease, Biochemistry 28 (1989) 8972–8979.

[36] I. Bertini, C. Luchinat, M. Piccioli, Paramagnetic probes in metalloproteins, Methods Enzymol. 339 (2001) 314–340.

[37] H. Cheng, J.L. Markley, NMR spectroscopic studies of paramagnetic proteins: iron–sulfur protein, Annu. Rev. Biophys. Biomol. Struct. 24 (1995) 209–237.

[38] J.R. Gillespie, D. Shortle, Characterization of long-range structure in the denatured state of staphylococcal nuclease: I. Paramagnetic relaxation enhancement by nitroxide spin labels, J. Mol. Biol. 268 (1997) 158–169.

[39] T. Mittag, J.D. Forman-Kay, Atomic-level characterization of disordered protein ensembles, Curr. Opin. Struct. Biol. 17 (2007) 3–14.

[40] D. Van der Spoel, E. Lindahl, B. Hess, G. Groenhof, A.E. Mark, H.J.C. Berendsen, GROMACS: fast, flexible, and free, J. Comp. Chem. 26 (2005) 1701–1718.

[41] G.A. Kaminski, R.A. Friesner, J. Tirado-Rives, W.L. Jorgensen, Evaluation and reparametrization of the OPLS-AA force field for proteins via comparison with accurate quantum chemical calculations on peptides, J. Phys. Chem., B 105 (2001) 6474–6487.

[42] H.J.C. Berendsen, J.P.M. Postma, W.F. van Gunsteren, J. Hermans, Interaction models for water in relation to protein hydration, Nature 224 (1969) 175–177.

[43] B. Hess, H. Bekker, H.J.C. Berendsen, J.G.E.M. Fraaije, LINCS: a linear constraint solver for molecular simulations, J. Comp. Chem. 18 (1997) 1463–1472.

[44] H.J.C. Berendsen, J.P.M. Postma, A. DiNola, J.R. Haak, Molecular dynamics with coupling to an external bath, J. Chem. Phys. 81 (1994) 3684–3690.
[45] T. Darden, D. York, L. Pedersen, Particle mesh Ewald: an *N*; log (*N*) method for Ewald sums in large systems, J. Chem. Phys. 98 (1993) 10089–10092.
[46] M. Akke, NMR methods for characterizing microseconds to millisecond dynamics in recognition and catalysis, Curr. Opin. Struct. Biol. 12 (2002) 642–647.
[47] C.R. Nakaie, S. Schreier, A.C. Paiva, Synthesis and properties of spin-labeled angiotensin derivatives, Biochim. Biophys. Acta 742 (1983) 63–71.
[48] C. Toniolo, M. Crisma, F. Formaggio, TOAC, a nitroxide spin-labeled, achiral Cα-tetrasubustituted α-amino acid, is an excellent tool in material science and biochemistry, Biopolymers 47 (1998) 153–158.
[49] J. García de la Torre, M.L. Huertas, B. Carrasco, HYDRONMR: prediction of NMR relaxation of globular proteins from atomic-level structures and hydrodynamic calculations, J. Magn. Reson. 147 (2000) 138–146.
[50] A.P. Valente, C.A. Miyamoto, F.C.L. Almeida, Implications of protein conformational diversity for binding and development of new biological active compounds, Curr. Med. Chem. 13 (2006) 3697–3703.
[51] J.N. Israelachvili, Intermolecular and Surface Forces, AcademicPress, London, 1992.
[52] L.C. James, D.S. Tawfik, Conformational diversity and protein evolution a 60-year-old hypothesis revised, Trends Biochem. Sci. 28 (2003) 361–368.
[53] M. Wolf-Watz, T. Grundstrom, T. Hard, Structure and backbone dynamics of Apo-CBFbeta in solution, Biochemistry 40 (2004) 11423–11432.
[54] L.C. James, D.S. Tawfik, Structure and kinetics of a transient antibody binding intermediate reveal a kinetic discrimination mechanism in antigen recognition, Proc. Natl. Acad. Sci. U. S. A. 6 (102) (2005) 12730–12735.
[55] M.R. Yeaman, N.Y. Yount, Mechanisms of antimicrobial peptide action and resistance, Pharmacol. Rev. 55 (2003) 27–55.
[56] J. Cavanagh, R.A. Venters, Protein dynamics studies move to a new time slot, Nat. Struct. Biol. 8 (2001) 912–914.
[57] K. Gunasekaran, R. Nussinov, How different are structurally flexible and rigid binding sites? Sequence and structural features discriminating proteins that do and do not undergo conformational change upon ligand binding, J. Mol. Biol. 365 (2007) 257–273.
[58] H.A. Carlson, J.A. McCammon, Accommodating protein flexibility in computational drug design, Mol. Pharmacol. 57 (2000) 213–218.
[59] M.J. Betts, M.J.E. Sternberg, An analysis of conformational changes on protein–protein association: implications for predictive docking, Protein Eng. 12 (1999) 271–283.
[60] M. Karplus, J. Janin, Comment on: "the entropy cost of protein association", Protein Eng. 12 (1999) 185–186.
[61] V.A. Jarymowycz, M.J. Stone, Fast time scale dynamics backbones: NMR relaxation methods, applications, and functional consequences, Chem. Rev. 106 (2006) 1624–1671.
[62] S.A. Dames, R. Aregger, N. Vajpai, P. Bernado, M. Blackledge, S. Grzesiek, Residual dipolar couplings in short peptides reveal systematic conformational preferences of individual amino acids, J. Am. Chem. Soc. 128 (2006) 13508–13514.
[63] B. Ma, T. Elkayam, H. Wolfson, R. Nussinov, Protein–protein interactions: structurally conserved residues distinguish between binding sites and exposed protein surfaces, Proc. Nat. Acad. Sci. 100 (2003) 5772–5777.
[64] F.C.L. Almeida, S.J. Opella, Measurement of H-1 T-1 rho in a uniformly N-15-labeled protein in solution with heteronuclear two-dimensional spectroscopy, J. Magn. Reson. 124 (1997) 509–511.
[65] B.F. Volkman, D. Lipson, D.E. Wemmer, D. Kern, Science two-state allosteric behavior in a single-domain signaling protein, Science 291 (2001) 2429–2433.
[66] A. Koglin, M.R. Mofid, F. Löhr, B. Schäfer, V.V. Rogov, M.M. Blum, T. Mittag, M.A. Marahiel, F. Bernhard, V.R. Dötsch, Conformational switches modulate protein interactions in peptide antibiotic synthetases, Science 312 (2006) 273–276.